ACADEMIC PRESS

Available online at www.sciencedirect.com

SCIENCE DIRECT®

Journal of Magnetic Resonance 164 (2003) 343–350

JMR Journal of Magnetic Resonance

www.elsevier.com/locate/jmr

Refocussing of chemical and paramagnetic shift anisotropies in ^{2}H NMR using the quadrupolar-echo experiment

Sasa Antonijevic and Stephen Wimperis*

School of Chemistry, University of Exeter, Stocker Road, Exeter EX4 4QD, UK

Received 31 March 2003; revised 23 July 2003

Abstract

A simple two-pulse spin-echo experiment is shown to refocus inhomogeneous broadening arising from both chemical and/or paramagnetic shift anisotropy and a first-order $I = 1$ quadrupolar interaction. The method is shown to yield ^{2}H NMR spectra of a paramagnetic solid ($CuCl_2 \cdot 2D_2O$) and of a non-paramagnetic solid ($D_2C_2O_4 \cdot 2D_2O$) that are significantly less distorted than those provided by the conventional quadrupolar-echo method. The technique will thus prove useful in studies of motion and dynamics where detailed analysis of the ^{2}H lineshape is performed.

1. Introduction

The recording of an NMR spectrum that contains a broad resonance presents certain practical difficulties. Simple ''pulse-acquire'' methods are unsatisfactory because the finite pulse duration and the ''deadtime'' between the end of the pulse and the start of data acquisition mean that each homogeneous component of the resonance has built up a frequency-dependent phase by the time of the first sampling point (this is shown schematically in Fig. 1a). A frequency-dependent linear combination of the real and imaginary components of the spectrum (a ''first-order phase correction'') provides an approximate method of correcting this phase error but the approximation is very poor for broad homogeneous components and/or large phase errors. If the broadening of the resonance is predominantly inhomogeneous then the most satisfactory method of recording an undistorted spectrum is to use a spin-echo method. At the echo maximum all homogeneous components of the broad resonance have the same phase and the experiment is readily performed such that this maximum lies within the data acquisition period, either coincident with the first sampling point (Fig. 1b) or with a much later sampling point such that a ''whole echo'' is acquired (Fig. 1c).

The choice of spin-echo method depends on the nature of the inhomogeneous broadening. If the broadening arises from terms in the free-precession Hamiltonian that are linear or effectively linear in the spin operators then a $90°_x$–τ–$180°_x$–τ– sequence, usually known as a Hahn [1] or Carr–Purcell (Method A) [2] echo, should be used. Examples of such broadening mechanisms include B_0 inhomogeneity, deliberate application of a B_0 gradient (as in NMR imaging or diffusion measurements) and — in powdered solids — chemical and paramagnetic shift anisotropies, heteronuclear dipolar interactions, and second-order quadrupolar interactions. In contrast, if the broadening arises from homonuclear dipolar interactions or from first-order quadrupolar interactions (i.e., from terms that are bilinear or quadratic in the spin operators) then a $90°_x$–τ–$90°_y$–τ– sequence should be used [3,4]. This pulse sequence is usually known as a solid or dipolar echo or, when used to refocus a first-order quadrupolar interaction, a quadrupolar echo. It is interesting to note, even in the recent literature, how often an inappropriate choice of spin-echo method is made.

Neither the conventional Hahn nor the conventional solid/dipolar/quadrupolar echo is appropriate if significant inhomogeneous broadening arises from more than one term in the Hamiltonian, at least one of which is linear

* Corresponding author. Fax: +44-1392-263434.
E-mail address: s.wimperis@exeter.ac.uk (S. Wimperis).

1090-7807/$ - see front matter © 2003 Elsevier Inc. All rights reserved.
doi:10.1016/S1090-7807(03)00272-6

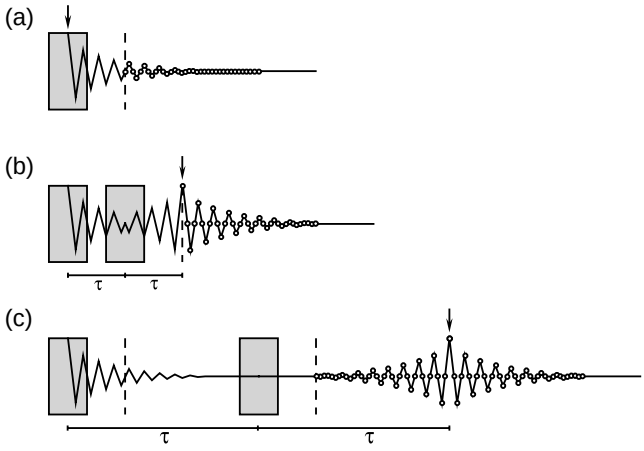

Fig. 1. Schematic data-acquisition methods for broad resonances: (a) simple "pulse-acquire" method; (b) spin-echo method with half-echo acquisition; (c) spin-echo method with whole-echo acquisition. The vertical dashed lines indicate the limit of the "deadtime" after the pulses during which data cannot be successfully sampled. The small circles represent data sampling points. The arrows indicate the point in the NMR signal where there is no frequency-dependent phase error: this point cannot be sampled in (a). If the homogeneous spin–spin relaxation time, T_2, permits its use, whole-echo acquisition in (c) yields a $\sqrt{2}$ increase in signal-to-noise ratio compared with half-echo acquisition in (b).

and one bilinear or quadratic. Such broadening is very common. The example we address here is that of ^{2}H ($I = 1$) NMR of solids, where the first-order quadrupolar interaction and the chemical and, in the case of paramagnetic solids, paramagnetic shift anisotropies combine to produce an inhomogeneous broadening that is often in excess of 250 kHz. In this paper we analyse the properties of the two spin-echo methods and show that simultaneous refocusing of linear and bilinear/quadratic interactions can be achieved in a simple two-pulse spin-echo experiment. This method is then used to yield undistorted ^{2}H NMR spectra of hydrated copper(II) chloride ($CuCl_2 \cdot 2D_2O$) and α-oxalic acid ($D_2C_2O_4 \cdot 2D_2O$).

2. Spin echoes and coherence transfer pathways

The density operator $\sigma(t)$ of an $I = 1$ spin system immediately after a 90°$_x$ pulse can be written

$$\sigma(0) = -I_y = -\mathrm{i}[T_{1,-1} + T_{1,+1}], \tag{1}$$

where we have used the normalized tensor operators $T_{l,p}$ of [5]. Free precession of this initial state for a period τ in the rotating frame under the influence of the (linear) offset Hamiltonian

$$H_{\mathrm{off}} = \Omega I_z \tag{2}$$

and the (quadratic) first-order quadrupolar Hamiltonian

$$H_{\mathrm{quad}} = \omega_{\mathrm{Q}}\left\{I_z^2 - \frac{I(I+1)}{3}\right\} \tag{3}$$

produces the following transformations:

$$\begin{aligned} &-\mathrm{i}[T_{1,-1} + T_{1,+1}] \\ &\xrightarrow{\Omega\tau} -\mathrm{i}[T_{1,-1}\exp\{\mathrm{i}\Omega\tau\} + T_{1,+1}\exp\{-\mathrm{i}\Omega\tau\}] \\ &\xrightarrow{\omega_{\mathrm{Q}}\tau} -\mathrm{i}[(T_{1,-1}\cos\omega_{\mathrm{Q}}\tau + \mathrm{i}T_{2,-1}\sin\omega_{\mathrm{Q}}\tau)\exp\{\mathrm{i}\Omega\tau\} \\ &\qquad + (T_{1,+1}\cos\omega_{\mathrm{Q}}\tau - \mathrm{i}T_{2,+1}\sin\omega_{\mathrm{Q}}\tau)\exp\{-\mathrm{i}\Omega\tau\}], \end{aligned} \tag{4}$$

where we used the shorthand "arrow notation" of [6]. Since $[H_{\mathrm{off}}H_{\mathrm{quad}}] = 0$, the order in which we do the transformations in Eq. (4) is irrelevant.

First, we consider the Hahn or Carr–Purcell (Method A) echo (Fig. 2a) [1,2] where a 180°$_x$ pulse is applied to the final state in Eq. (4) and a spin echo is formed following a second period τ of free precession:

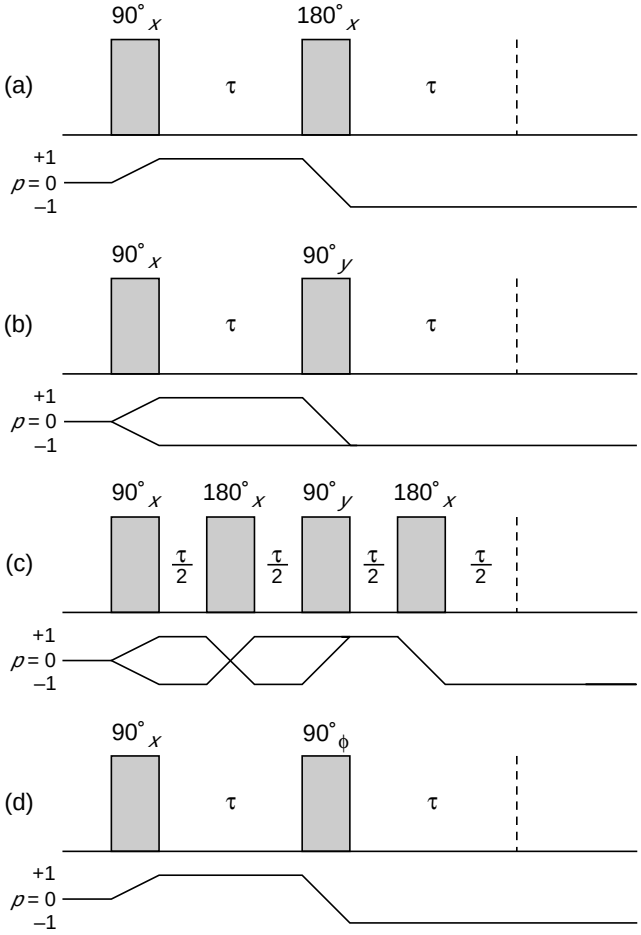

Fig. 2. Spin-echo pulse sequences and associated coherence transfer pathways: (a) Hahn or Carr–Purcell (Method A) echo; (b) conventional quadrupolar echo; (c) quadrupolar-echo sequence of Siminovitch et al. [12]; (d) single-pathway, "Exorcycled" quadrupolar echo. Phase cycles are given in Table 1. The spin-echo sequences in (c) and (d) achieve simultaneous refocussing of chemical and/or paramagnetic shift anisotropy and the first-order quadrupolar interaction.

$$
\begin{aligned}
&- \mathrm{i}[(T_{1,-1}\cos\omega_Q\tau + \mathrm{i}T_{2,-1}\sin\omega_Q\tau)\exp\{\mathrm{i}\Omega\tau\} \\
&\quad + (T_{1,+1}\cos\omega_Q\tau - \mathrm{i}T_{2,+1}\sin\omega_Q\tau)\exp\{-\mathrm{i}\Omega\tau\}] \\
\overset{180°_x}{\rightarrow} &- \mathrm{i}[(-T_{1,+1}\cos\omega_Q\tau + \mathrm{i}T_{2,+1}\sin\omega_Q\tau)\exp\{\mathrm{i}\Omega\tau\} \\
&\quad + (-T_{1,-1}\cos\omega_Q\tau - \mathrm{i}T_{2,-1}\sin\omega_Q\tau)\exp\{-\mathrm{i}\Omega\tau\}] \\
\overset{\Omega\tau}{\rightarrow} &- \mathrm{i}[(-T_{1,+1}\cos\omega_Q\tau + \mathrm{i}T_{2,+1}\sin\omega_Q\tau) \\
&\quad + (-T_{1,-1}\cos\omega_Q\tau - \mathrm{i}T_{2,-1}\sin\omega_Q\tau)] \qquad (5) \\
\overset{\omega_Q\tau}{\rightarrow} &- \mathrm{i}[(-T_{1,+1}\cos^2\omega_Q\tau + \mathrm{i}T_{2,+1}2\sin\omega_Q\tau\cos\omega_Q\tau \\
&\quad + T_{1,+1}\sin^2\omega_Q\tau) \\
&\quad + (-T_{1,-1}\cos^2\omega_Q\tau - \mathrm{i}T_{2,-1}2\sin\omega_Q\tau\cos\omega_Q\tau \\
&\quad + T_{1,-1}\sin^2\omega_Q\tau)] \\
&= +\mathrm{i}(T_{1,-1}+T_{1,+1})\cos 2\omega_Q\tau \\
&\quad - (T_{2,-1}-T_{2,+1})\sin 2\omega_Q\tau \\
&= \sigma(2\tau).
\end{aligned}
$$

Thus, the density operator at the end of the second free-precession period, $\sigma(2\tau)$, is modulated as a function of 2τ only by the quadrupolar splitting parameter ω_Q and not by the offset Ω. A 180° pulse transforms all $p=-1$ operators/coherences exclusively to $p=+1$ operators/coherences (and vice versa) and it is this change in the sign of the coherence order p that leads to refocussing of the offset Ω. However, a 180° pulse leaves the relative signs of $T_{1,p}$ and $T_{2,p}$ operators unchanged and, hence, cannot refocus the first-order quadrupolar interaction.

Quadrature detection of the NMR signal, $s(t)$, in the rotating frame means that only one of the two counter-rotating components represented by coherence orders $p=+1$ and $p=-1$ is detected. By convention [7], quadrature detection corresponds to taking the trace of the product of the density operator and the $T_{1,+1}$ operator, i.e.,

$$s(t) = \mathrm{Tr}\{\sigma(2\tau+t)T_{1,+1}\} \qquad (6)$$

and so, because of the orthogonality condition $\mathrm{Tr}\{T_{l,p}T_{l',p'}\} = (-1)^p\delta_{l',l}\delta_{p,-p'}$, only $p=-1$ components of the density operator $\sigma(2\tau)$ can be observed during the data acquisition period. Thus we can write the observable part of $\sigma(2\tau)$ in Eq. (5) as

$$\sigma^{p=-1}(2\tau) = +\mathrm{i}T_{1,-1}\cos 2\omega_Q\tau - T_{2,-1}\sin 2\omega_Q\tau. \qquad (7)$$

The coherence transfer pathway [7] drawn below the Hahn-echo sequence in Fig. 2a serves as a shorthand reminder that, after the 180° pulse, only $p=-1$ coherences are observable but that, during the first τ period, because of the change in sign of p produced by the 180° pulse, these same coherences had order $p=+1$.

Second, we consider the conventional quadrupolar echo (Fig. 2b) [4] where a $90°_y$ pulse is applied to the final state in Eq. (4) and a spin echo is formed following a second period τ of free precession:

$$
\begin{aligned}
&- \mathrm{i}[(T_{1,-1}\cos\omega_Q\tau + \mathrm{i}T_{2,-1}\sin\omega_Q\tau)\exp\{\mathrm{i}\Omega\tau\} \\
&\quad + (T_{1,+1}\cos\omega_Q\tau - \mathrm{i}T_{2,+1}\sin\omega_Q\tau)\exp\{-\mathrm{i}\Omega\tau\}] \\
\overset{90°_y}{\rightarrow} &- \mathrm{i}\left[\left(\frac{1}{2}T_{1,-1}\cos\omega_Q\tau - \frac{\mathrm{i}}{2}T_{2,-1}\sin\omega_Q\tau\right)\exp\{\mathrm{i}\Omega\tau\}\right. \\
&\quad \left. + \left(\frac{1}{2}T_{1,-1}\cos\omega_Q\tau - \frac{\mathrm{i}}{2}T_{2,-1}\sin\omega_Q\tau\right)\exp\{-\mathrm{i}\Omega\tau\}\right] \\
\overset{\Omega\tau}{\rightarrow} &- \frac{\mathrm{i}}{2}[(T_{1,-1}\cos\omega_Q\tau - \mathrm{i}T_{2,-1}\sin\omega_Q\tau)\exp\{\mathrm{i}2\Omega\tau\} \\
&\quad + (T_{1,-1}\cos\omega_Q\tau - \mathrm{i}T_{2,-1}\sin\omega_Q\tau)] \qquad (8) \\
\overset{\omega_Q\tau}{\rightarrow} &- \frac{\mathrm{i}}{2}\big[\big(T_{1,-1}\cos^2\omega_Q\tau + \mathrm{i}T_{2,-1}\sin\omega_Q\tau\cos\omega_Q\tau \\
&\quad - \mathrm{i}T_{2,-1}\sin\omega_Q\tau\cos\omega_Q\tau + T_{1,-1}\sin^2\omega_Q\tau\big) \\
&\quad \times \exp\{\mathrm{i}2\Omega\tau\} \\
&\quad + \big(T_{1,-1}\cos^2\omega_Q\tau + \mathrm{i}T_{2,-1}\sin\omega_Q\tau\cos\omega_Q\tau \\
&\quad - \mathrm{i}T_{2,-1}\sin\omega_Q\tau\cos\omega_Q\tau + T_{1,-1}\sin^2\omega_Q\tau\big)\big] \\
&= -\frac{\mathrm{i}}{2}[T_{1,-1}\exp\{\mathrm{i}2\Omega\tau\} + T_{1,-1}] \\
&= \sigma^{p=-1}(2\tau).
\end{aligned}
$$

(Note that we have simplified this calculation with respect to that in Eq. (5) by retaining only $p=-1$ operators after the $90°_y$ pulse, i.e., those operators that will be observable during the data acquisition period.) Thus, for the quadrupolar echo, the density operator $\sigma(2\tau)$ is modulated as a function of 2τ only by the offset Ω and not by the quadrupolar splitting parameter ω_Q. The $90°_y$ pulse changes the relative signs of $T_{1,p}$ and $T_{2,p}$ operators and, hence, refocusses the first-order quadrupolar interaction but transforms both $p=+1$ and $p=-1$ operators into observable $p=-1$ operators and so does not refocus the offset Ω. The coherence transfer pathways drawn below the sequence in Fig. 2b are now a reminder that both $p=+1$ and $p=-1$ coherences during the first τ period contribute to the observable $p=-1$ coherences after the $90°_y$ pulse.

In addition to depicting which coherence orders present during the pulse sequence contribute to the final observable signal, the main purpose of drawing a coherence transfer pathway diagram is that it *specifies the phase cycle that must be used* [7,8]. If, for example, the 90° and 180° pulses in the Hahn-echo sequence in Fig. 2a were perfect then no phase cycling would be necessary in this experiment. In reality, however, two pulse imperfections are universally encountered: (i) the B_1 radiofrequency field is inhomogeneous; and (ii) $\omega_1 = -\gamma B_1$ never fulfills the "ideal" conditions $\omega_1 \gg \Omega$ and $\omega_1 \gg \omega_Q$, especially the latter [9]. Therefore, $p=0$ and -1 coherences will inevitably be present during the first τ period in Fig. 2a and, unless phase cycling is used, will make a deleterious contribution to the observable signal (i.e., they will yield signal components that are modulated by Ω as a

function of 2τ). Correct phase cycling of the 90° and 180° pulses allows us, in effect, to block the unwanted $p = 0$ and -1 coherences and to select only the *desired* pathway (the one shown below the pulse sequence in Fig. 2a), thereby ensuring that $\sigma^{p=-1}(2\tau)$ is not modulated by the offset Ω.

Although shorter phase cycles (and even some provided by spectrometer manufacturers) may be satisfactory, rigorous application of the rules of phase cycling [7,8] to the Hahn-echo coherence transfer pathway in Fig. 2a suggests the following two components of a complete phase cycle: (i) selection of a change in coherence order, Δp, of -2 by the 180° pulse using a 4-step phase cycle (known as "Exorcycle" [10]) or, if non-90° phase shifts can be used, a 3-step phase cycle [7]; and (ii), as is usual whenever quadrature detection is used, a 4-step phase cycle (known as CYCLOPS [11]) of both pulses simultaneously that selects $\Delta p = -1$ over the whole sequence. Nesting of CYCLOPS with the 4-step Exorcycle produces a 16-step phase cycle, while a 12-step phase cycle results if the 3-step alternative to Exorcycle is used. Both of these complete phase cycles are listed in Table 1. In a similar fashion, pulse imperfections mean that phase cycling of the quadrupolar-echo sequence is necessary (to block $p = 0$ during the first τ period) and application of the phase cycling rules to the coherence transfer pathways in Fig. 2b suggests the following: (i) selection of a change in coherence order $\Delta p = 0$ *and* -2 by the second 90° pulse using a 2-step phase cycle; and (ii) CYCLOPS of both pulses simultaneously. The resulting 8-step phase cycle is also given in Table 1.

3. Simultaneous refocussing of offsets and quadrupolar splittings

Eqs. (5) and (8) confirm that neither the conventional Hahn-echo nor the conventional quadrupolar echo is appropriate if inhomogeneous broadening arises in ^{2}H NMR from both chemical and/or paramagnetic shift anisotropy (exemplified above by the offset Ω) and a first-order quadrupolar interaction. Siminovitch et al. have proposed the pulse sequence in Fig. 2c for simultaneous refocussing of both types of interaction [12]. The $90°_y$ pulse refocusses the first-order quadrupolar interaction (as in a conventional quadrupolar echo) while the 180° pulses positioned in the middle of the two τ periods ensure that there is no net offset evolution (as in a Hahn echo). The observable part of the density operator at the end of the second τ period is given by

$$\sigma^{p=-1}(2\tau) = -\mathrm{i}T_{1,-1} \tag{9}$$

and thus, as desired, is purely rank $l = 1$ and modulated by neither the offset Ω nor the quadrupolar splitting parameter ω_Q. The phase cycling rules [7,8] suggest four components of a complete phase cycle: (i) a 4-step Exorcycle of the first 180° pulse to select $\Delta p = \pm 2$; (ii) a 2-step phase cycle of the second 90° pulse to select $\Delta p = 0$ and +2; (iii) a 4-step Exorcycle (or the 3-step alternative) of the second 180° pulse to select $\Delta p = -2$; and (iv) CYCLOPS of all four pulses simultaneously. Although totally successful in its refocussing aims, the Siminovitch sequence has the disadvantage that four pulses with a total rotation angle of 540° are required (compared with 270° for the Hahn echo and 180° for the quadrupolar

Table 1
Phase cycles for spin-echo pulse sequences in Fig. 2 (with $0° = x$, $90° = y$, $180° = -x$, $270° = -y$)

(A) *16-step phase cycle (CYCLOPS + Exorcycle) for Hahn/Carr–Purcell (Method A) echo (Fig. 2a) or single-pathway quadrupolar echo (Fig. 2d)*								
First pulse	0°	90°	180°	270°	0°	90°	180°	270°
	0°	90°	180°	270°	0°	90°	180°	270°
Second pulse	0°	90°	180°	270°	90°	180°	270°	0°
	180°	270°	0°	90°	270°	0°	90°	180°
Receiver	0°	90°	180°	270°	180°	270°	0°	90°
	0°	90°	180°	270°	180°	270°	0°	90°
(B) *12-step phase cycle (CYCLOPS + 3-step alternative to Exorcycle) for Hahn/Carr–Purcell (Method A) echo (Fig. 2a) or single-pathway quadrupolar echo (Fig. 2d)*								
First pulse	0°	90°	180°	270°	120°	210°	300°	30°
	240°	330°	60°	150°				
Second pulse	0°	90°	180°	270°	240°	330°	60°	150°
	120°	210°	300°	30°				
Receiver	0°	90°	180°	270°	0°	90°	180°	270°
	0°	90°	180°	270°				
(C) *8-step phase cycle (CYCLOPS + 2-step cancellation of $p = 0$) for conventional quadrupolar echo (Fig. 2c)*								
First pulse	0°	90°	180°	270°	0°	90°	180°	270°
Second pulse	90°	180°	270°	0°	270°	0°	90°	180°
Receiver	0°	90°	180°	270°	0°	90°	180°	270°

echo) and, since ω_Q^{max} is typically in the range 75–150 kHz, this places very high demands on the value of $\omega_1 = -\gamma B_1$ that must be achieved by the NMR probe and amplifiers if severely distorted ^{2}H spectra are to be avoided.

In this paper we propose the two-pulse pulse sequence in Fig. 2d for simultaneous refocussing of shift anisotropy and first-order quadrupolar interactions in ^{2}H NMR. (This sequence has appeared in a number of guises over the last 20 or so years [13–15] but never, to our knowledge, in this particular application.) Inspection of the final density operator, $\sigma^{p=-1}(2\tau)$, in the conventional quadrupolar-echo sequence in Eq. (8) shows that it consists of two $T_{1,-1}$ terms, one that is modulated by the offset Ω as a function of 2τ and one that is not. As in the Hahn echo, the latter $p = -1$ term arises from operators that had coherence order $p = +1$ during the first τ period. Therefore, by using phase cycling to block the $p = -1$ pathway during the first τ period and to select just the coherence transfer pathway shown in Fig. 2d, one obtains the observable part of the density operator at the end of the second τ period

$$\sigma^{p=-1}(2\tau) = -\frac{i}{2} T_{1,-1} \tag{10}$$

and, as required, this is modulated by neither the offset Ω nor the quadrupolar splitting parameter ω_Q. In practice, all that is needed is that the 12- or 16-step phase cycle derived for the Hahn echo and given in Table 1 be applied to the quadrupolar-echo sequence. Comparison of Eqs. (9) and (10) shows that this Exorcycled quadrupolar-echo sequence has the disadvantage of yielding only half the signal amplitude of the Siminovitch sequence (because the phase cycling has removed half of the signal) but, as will be shown below, has two considerable advantages: (i) spectra with only minimal distortion can be obtained using only moderate pulse powers; and (ii) because the second τ period is not interrupted by a 180° pulse, shorter τ periods can be accessed.

4. Results

We have investigated the ability of the conventional quadrupolar-echo, Siminovitch and Exorcycled quadrupolar-echo sequences to yield undistorted ^{2}H powder-pattern spectra using computer simulation. Our home-written program calculates the rotating-frame evolution of the spin $I = 1$ density matrix under a series of finite duration pulses and free-precession intervals, and uses exact numerical diagonalization of the full pulse Hamiltonian. The free-precession Hamiltonian includes both a first-order quadrupolar interaction and a shift anisotropy. The trace of the product of $\sigma(2\tau + t)$ with $T_{1,+1}$ yields the time-domain signal $s(t)$ and this is Fourier transformed to provide the spectrum.

Fig. 3 shows the resulting half-echo spectra simulated with both an unrealistically high radiofrequency field strength ($\omega_1/2\pi = 1$ MHz) and a more readily achievable value ($\omega_1/2\pi = 100$ kHz). With the high value of ω_1, both the Siminovitch and Exorcycled quadrupolar-echo sequences yield an essentially undistorted powder lineshape (a skewed Pake doublet [16] characteristic of the presence of a significant shift anisotropy) and, as predicted, the latter yields precisely half the signal intensity of the former. In contrast, the conventional quadrupolar-echo sequence yields a highly distorted

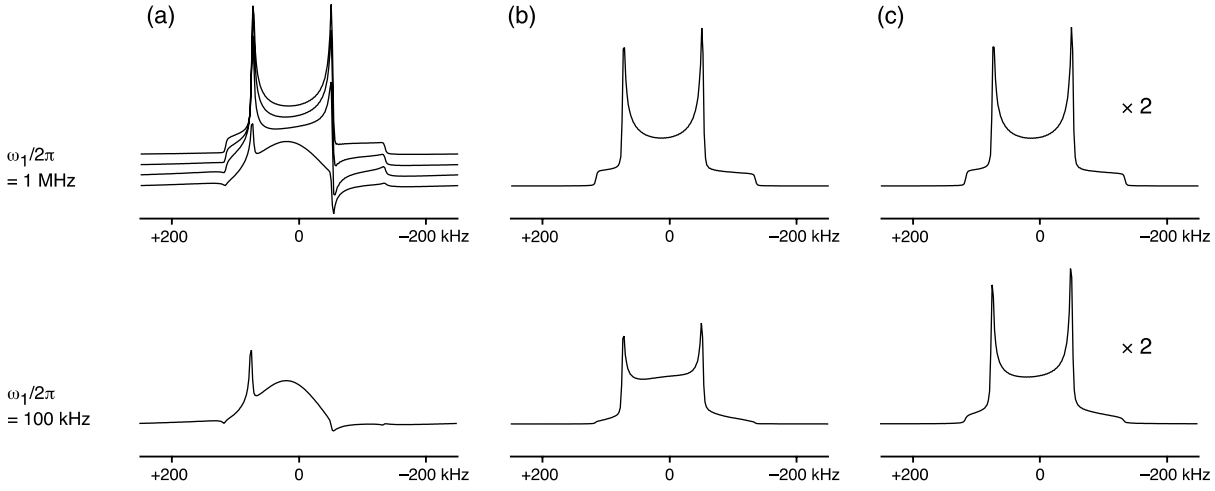

Fig. 3. Computer simulations of half-echo spectra yielded by (a) conventional quadrupolar echo, (b) quadrupolar-echo sequence of Siminovitch et al. [12], and (c) single-pathway, Exorcycled quadrupolar echo. The maximum quadrupolar splitting parameter, $\omega_Q^{max}/2\pi$, was 125 kHz, the quadrupolar asymmetry parameter, η_Q, was 0, and the three principal components of the shift anisotropy tensor (assumed to be coaxial with the quadrupolar interaction tensor) were $\omega_{x,x}/2\pi = \omega_{y,y}/2\pi = 10$ kHz and $\omega_{z,z}/2\pi = -10$ kHz. Two radiofrequency field strengths were used, corresponding to $\omega_1/2\pi = -\gamma B_1/2\pi = 1$ MHz (a 90° pulse duration of 0.25 μs) and $\omega_1/2\pi = 100$ kHz (a 90° pulse duration of 2.5 μs), as shown. The τ period was 20 μs in each case, except in (a) with $\omega_1/2\pi = 1$ MHz, where τ periods of 2.5, 5, 10, and 20 μs were used.

spectrum that is a function of τ, showing that simultaneous refocussing of the two broadening interactions has not been achieved. With the more realistic value of ω_1, the Siminovitch sequence produces a spectrum that has lost significant overall intensity (reduced by 37% in the "horns") and is also now quite distorted, especially in the "shoulders" of the Pake pattern, while the Exorcycled quadrupolar echo yields a spectrum that is less distorted and also retains a greater fraction of its original intensity (reduced by less than 2% in the horns).

Experimental investigations of the three quadrupolar-echo sequences were performed on a Bruker Avance 400 spectrometer equipped with a widebore 9.4 T magnet. Using a 1 kW radiofrequency amplifier and a 4-mm coil, we obtained a 90° pulse duration of 1.8 μs ($\omega_1/2\pi = 140$ kHz) at the ^{2}H Larmor frequency of $\omega_0/2\pi = 61.4$ MHz. All τ periods were corrected for finite pulse durations, as shown in Fig. 1 [9].

Fig. 4 shows the resulting ^{2}H NMR spectra of copper(II) chloride dihydrate ($CuCl_2 \cdot 2D_2O$). The copper(II) ion is responsible for the presence of a significant paramagnetic shift anisotropy (PSA), while the lineshape is also motionally averaged by a rapid reorientation of the heavy water molecules about the bisectors of their D–O–D angles [17,18]. With a τ period of 30 μs, only the Exorcycled quadrupolar-echo sequence yields an undistorted spectrum, since the Siminovitch sequence produces a poor baseline as a result of the final free-precession period, $\tau/2 = 15$ μs, ending within the instrumental deadtime. On lengthening the τ period to 60 μs, the Siminovitch sequence appears to yield an undistorted spectrum but careful examination shows that, as a result of finite pulse duration effects, the shoulders of the powder-pattern lineshape are not as distinct as those in the Exorcycled quadrupolar-echo spectrum. As expected, with a τ period of either 30 or 60 μs, the conventional quadrupolar-echo sequence yields a highly distorted spectrum owing to the failure to refocus the shift anisotropy. In contrast to the $\tau = 30$ and 60 μs spectra, the Exorcycled quadrupolar-echo spectrum recorded with $\tau = 100$ μs is a whole-echo spectrum (see Fig. 1c). If the T_2 spin–spin relaxation time permits its use (as here), this method of acquisition has the advantage of yielding a factor of 2 in signal (S) at the cost of a factor of $\sqrt{2}$ in noise (N), hence a factor of $\sqrt{2}$ in S/N [19], and of providing a very flat baseline. When correctly phased, whole-echo spectra have no imaginary component and thus can be easily and accurately phased by using this as the criterion.

Even in non-metallic, non-paramagnetic, uniformly powdered solids where, in addition to the first-order quadrupolar interaction, only the chemical shift anisotropy (CSA) is present, the Exorcycled quadrupolar-echo sequence will still yield less distorted spectra than the conventional sequence. Fig. 5 shows ^{2}H NMR spectra of α-oxalic acid dihydrate ($D_2C_2O_4 \cdot 2D_2O$). The

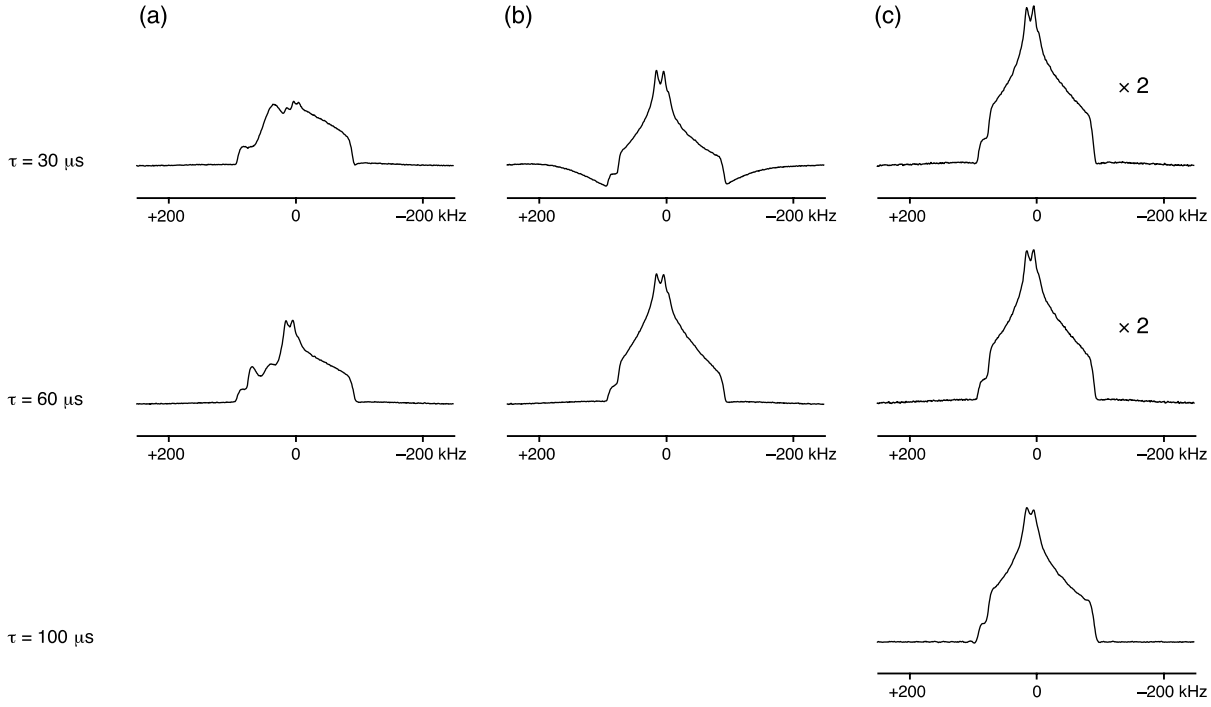

Fig. 4. Half- and whole-echo ^{2}H ($\omega_0/2\pi = 61.4$ MHz) spectra of $CuCl_2 \cdot 2D_2O$ yielded by (a) conventional quadrupolar echo (8-step phase cycle), (b) quadrupolar-echo sequence of Siminovitch et al. (128-step phase cycle), and (c) single-pathway, Exorcycled quadrupolar echo (16-step phase cycle). A radiofrequency field strength corresponding to $\omega_1/2\pi = 140$ kHz (a 90° pulse duration of 1.8 μs) was used and 1024 transients were averaged with a relaxation interval of 0.5 s. The duration of the data acquisition period was 0.512 ms in each case and no weighting functions were applied. The τ periods used were 30 μs (half-echo acquisition), 60 μs (half-echo acquisition), and 100 μs (whole-echo acquisition), as shown.

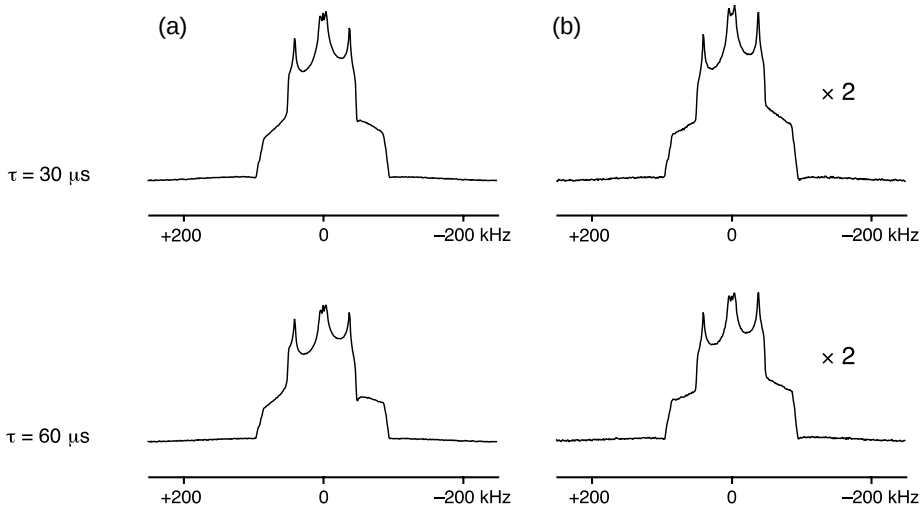

Fig. 5. Half-echo ^2H ($\omega_0/2\pi = 61.4$ MHz) spectra of $D_2C_2O_4 \cdot 2D_2O$ yielded by (a) conventional quadrupolar echo (8-step phase cycle) and (b) single-pathway, Exorcycled quadrupolar echo (16-step phase cycle). A radiofrequency field strength corresponding to $\omega_1/2\pi = 140$ kHz (a 90° pulse duration of 1.8 μs) was used and 1024 transients were averaged with a relaxation interval of 0.5 s. The duration of the data acquisition period was 0.512 ms in each case and no weighting functions were applied. The τ periods used were 30 and 60 μs, as shown.

spectra are the superposition of a typical Pake doublet arising from the oxalic acid deuterons and a motionally averaged lineshape arising from the deuterons in the water molecules, which are undergoing rapid reorientation [20,21]. There is an isotropic chemical shift difference of 11 ppm (or 680 Hz on our 9.4 T magnet) between the two powder patterns (determined from the ^1H and ^2H MAS spectra). Comparison of the spectra yielded by the conventional and Exorcycled quadrupolar-echo sequences reveals that the shoulders of the former have a significant τ-dependent distortion that is absent in the latter.

5. Conclusions

Both the Siminovitch quadrupolar echo in Fig. 2c and the Exorcycled quadrupolar echo in Fig. 2d are useful methods of recording ^2H NMR spectra that are broadened by both first-order quadrupolar interactions and shift anisotropies. The latter technique has the disadvantage that, under ideal conditions, it yields half the signal-to-noise ratio of the Siminovitch sequence. However, we have shown that the Exorcycled quadrupolar echo has the following advantages: (i) spectra with only minimal distortion can be obtained using only moderate pulse powers; and (ii) because the second τ period is not interrupted by a 180° pulse, shorter τ periods can be accessed. We have also shown that, as a consequence of point (ii), the Exorcycled quadrupolar-echo sequence is readily compatible with whole-echo acquisition and that, where applicable, this felicitous approach provides flat baselines and a $\sqrt{2}$ relative increase in signal-to-noise ratio. Although demonstrated here in ^2H NMR spectroscopy, we believe that the Exorcycled solid/dipolar/quadrupolar echo will prove useful wherever broadening arises from both linear (e.g., the Knight shift) and bilinear/quadratic interactions (e.g., the homonuclear dipolar coupling).

Acknowledgments

We are grateful to EPSRC for generous support (Grant No. GR/N07622) and to Dr. John Welch for his preliminary work on this project.

References

[1] E.L. Hahn, Phys. Rev. 80 (1950) 580.
[2] H.Y. Carr, E.M. Purcell, Phys. Rev. 94 (1954) 630.
[3] B.C. Gerstein, in: D.M. Grant, R.K. Harris (Eds.), Encyclopedia of Nuclear Magnetic Resonance, vol. 3, Wiley, Chichester, 1996, p. 1835.
[4] J.H. Davis, K.R. Jeffrey, M. Bloom, M.I. Valic, T.P. Higgs, Chem. Phys. Lett. 42 (1976) 390.
[5] N. Müller, G. Bodenhausen, R.R. Ernst, J. Magn. Reson. 75 (1987) 297.
[6] O.W. Sørensen, G.W. Eich, M.H. Levitt, G. Bodenhausen, R.R. Ernst, Prog. NMR Spectrosc. 16 (1983) 163.
[7] G. Bodenhausen, H. Kogler, R.R. Ernst, J. Magn. Reson. 58 (1984) 370.
[8] P.J. Hore, J.A. Jones, S. Wimperis, NMR: The Toolkit, Oxford University Press, Oxford, 2000 (Chapter 6).
[9] M. Bloom, J.H. Davis, M.I. Valic, Can. J. Phys. 58 (1980) 1510.
[10] G. Bodenhausen, R. Freeman, D.L. Turner, J. Magn. Reson. 27 (1977) 511.
[11] D.I. Hoult, R.E. Richards, Proc. Roy. Soc. (London) A344 (1975) 311.
[12] D.J. Siminovitch, M. Rance, K.R. Jeffrey, M.F. Brown, J. Magn. Reson. 58 (1984) 62.
[13] R.L. Vold, R.R. Vold, J. Magn. Reson. 42 (1981) 173.

[14] I. Furó, B. Halle, J. Magn. Reson. 98 (1992) 388.
[15] I. Furó, N. Hedin, J. Magn. Reson. 152 (2001) 214.
[16] G.E. Pake, J. Chem. Phys. 16 (1948) 327.
[17] T.-H. Lin, J.A. DiNatale, R.R. Vold, J. Am. Chem. Soc. 116 (1994) 2133.
[18] J.A. DiNatale, R.R. Vold, J. Magn. Reson. 117 (1995) 304.
[19] P.T. Callaghan, Principles of Nuclear Magnetic Resonance Microscopy, Clarendon Press, Oxford, 1991 (Chapter 2).
[20] L. Zheng, K.W. Fishbein, R.G. Griffin, J. Herzfeld, J. Am. Chem. Soc. 115 (1993) 6254.
[21] S.E. Ashbrook, S. Antonijevic, A.J. Berry, S. Wimperis, Chem. Phys. Lett. 364 (2002) 634.